



CHAPTER II

Theoretical Background and Literature Review

2.1. Plasma Source Ion Implant^[1, 2, 3]

Plasma is the fourth state of the matter that state is ion and electron can stay simultaneously but they are not combinable. When solid is heated enough the atom break the crystal lattice structure, a liquid is formed. When liquid is heated enough that atoms vaporize off the surface faster than they do recon dense, a gas is formed. When a gas is heated further, the atoms collide with each other and knock their electrons off in the process, a plasma formed.

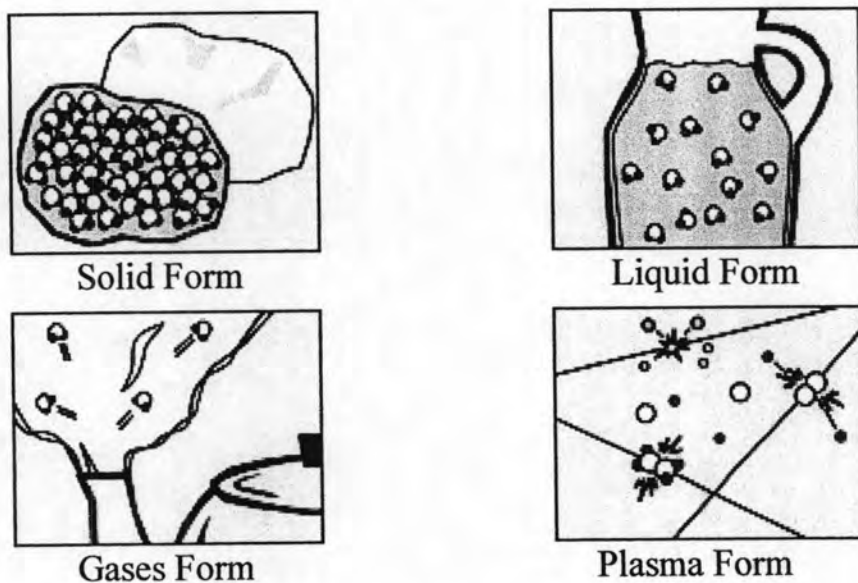


Fig. 2.1 State of the matter

In 1978s, J. R. Conrad^[4] developed an innovative and cost effective ion implant technique, which was called plasma source ion implantation (PSII). It has been optimized for the surface modification of material such as metal plastics, and ceramic. PSII departs radically from conventional implantation technology by circumventing the line-of-sight restriction inherent in conventional ion implantation.

PSII techniques, offers a number of advantages relative to other surface modification techniques: (1) Surface properties can be changed selectively without changing desirable bulk material properties. (2) There are no problems associated with bonding failure or surface layer delaminating (3) since ion implantation is not a “coating” process, there are no associated dimensional changes in the work piece; cutting edges retain their sharpness. (4) The implant species concentration profile can be easily changed by changing the thermodynamic properties and diffusion kinetics. (5) Ion implantation is a low-temperature process; there are no (or minimal) dimensional changes due to thermal distortion; there is no (or minimal) degradation of surface finish.

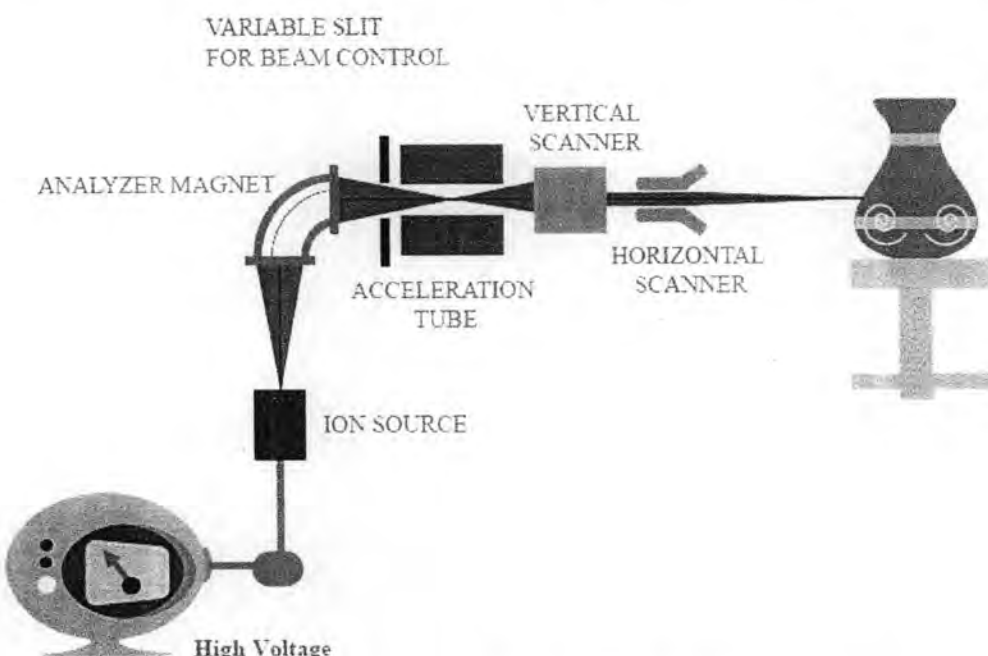


Fig. 2.2 Schematic of conventional ion implantation

Plasma source ion implantation (PSII) is one of several methods for process plasma. This process, coating ions are accelerated to high energy and injected into the surface of the target, resulting in the modified surface layer. Recently, Plasma source ion implantation technique has been used to modify the materials surface for example to improve the wear resistance of metal. It has been well known that nitrogen ion implantation on the tool steel gives significant improvement of the wear property.

Plasma Source Ion Implantation (PSII) is a room temperature, Plasma-based, surface enhancement technology that uses an ionized gas surrounding a target and high-negative-voltage, high-current pulses to accelerate ions into a target surface from all directions. Ion implantation can modify the target surface in beneficial ways, making it harder, reducing the coefficient of friction, and enhancing its resistance to corrosion. These benefits are similar to those obtained through conventional ion beam implantation but PSII differs from conventional techniques in several important aspects.

In plasma source ion implantation (PSII), the target is placed directly in the plasma chamber and is repetitively pulse-biased to a high negative voltage relative to the vacuum chamber walls, which is electrically grounded. During the high voltage pulses, dynamic plasma sheath is formed around the target and the ions from the plasma or coating material are accelerated normal and driven into the target object surfaces from all sides simultaneously. They are implanted with the energy corresponding to the applied voltage. The target manipulation is not necessary because the plasma surrounds the target completely and all exposed surface of the target is implanted simultaneously.

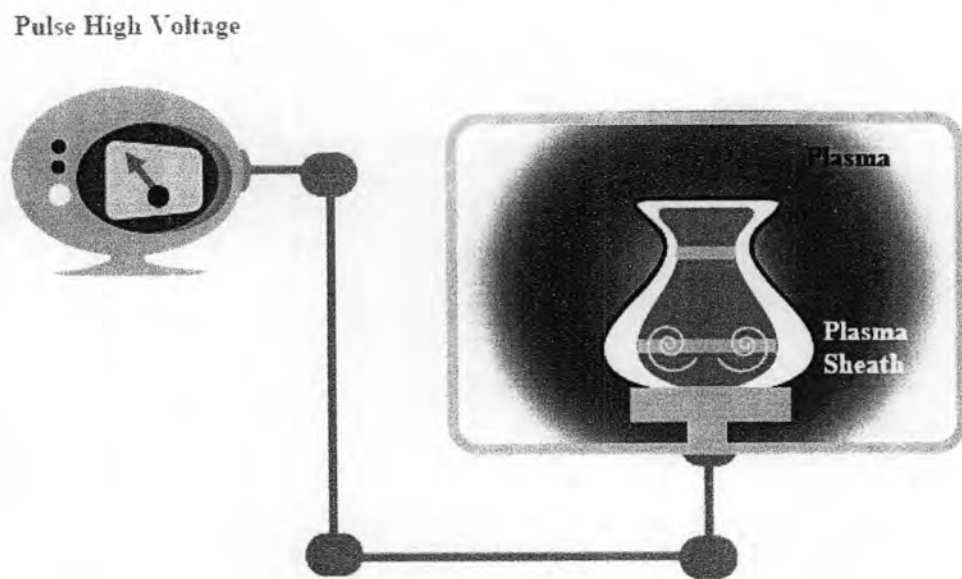


Fig. 2.3 Schematic of plasma source ion implantation (PSII) process

There are two types of plasma model for simulated the phenomena. First model is particle model and second model is fluid model. Therefore, the plasma coatings have two models too. The model of plasma source ion implantation can simulate the process of coating and predict the result of coating.

Particle Model: This involves following the motion of large number of charged particles in their self-consistent electric fields. It is limited to only simulated the phenomenon in which only a small fraction of plasma is involved and only for a short period.

Fluid Model: This adopts a set of the fluid equation to describe by solving numerically the magneto hydrodynamic equation. The method is possible because of the fact that plasma behaves sometime like a fluid and sometime like a collection of individual particles. In the fluid approximate, plasma is considered to compose of two or more interpenetrating fluids. By treating plasma as a magnetized conducting fluid, this method can be applied to the large-scale problem. In this research, however the Particle model is employed due to its simplicity and the direct application on the process of coating.

2.2 Theory of Plasma^[2]

2.2.1 Criteria of plasma

A. Debye Shield

A fundamental characteristic of the behavior of plasma is its ability to shield out electric potential that are applied to it. Supposed this idea tried to put an electric field inside plasma by inserting two charged balls connected to a battery, Figure 2.4. The balls would attract particles of the opposite charge, and almost immediately a cloud of ions would surround the negative ball and cloud of electrons would surround the positive ball. (The theory assumes that a layer of dielectric keeps the plasma from actually recombining on the surface, or that the battery is large enough to maintain the potential in spite of this.) If the plasma were cold and there were no thermal motions, there would be just as many charges in the cloud as in the ball; the shielding would be perfect, and no electric field would be present in the body of the plasma out side the clouds. On the other

hand, if the temperature is finite, those particles that are at the edge of the cloud, where the electric field is weak, have enough thermal energy to escape from the electrostatic potential well. The “edge” of the cloud that occurs at the radius where the potential energy is approximately equal to the thermal energy $K_B T$ of the particles, and the shielding is not complete. Potentials of the order of $\frac{K_B T}{e}$ can leak into the plasma and cause finite electric field to exist there.

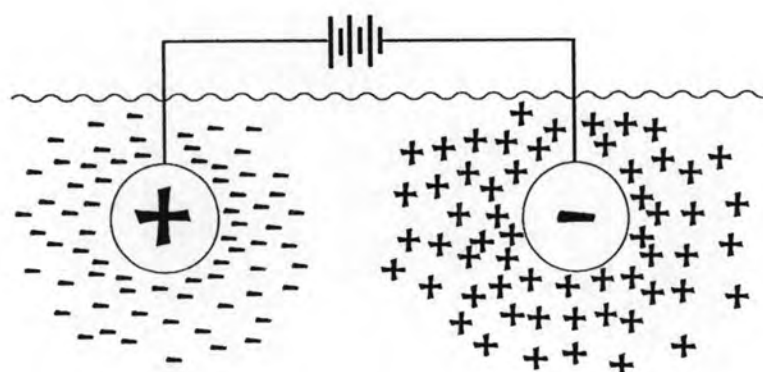


Fig. 2.4 Debye Shield

Debye Shield is a fundamental characteristic of the behavior of plasma is its ability to shield out electric potentials that are applied to it. The Debye shielding is a sphere and the radius size can be defined by

$$\lambda_D = \left(\frac{\epsilon_0 K_B T}{mq^2} \right)^{1/2} \quad (2.1)$$

For λ_D = Debye Shield radius (m)

ϵ_0 = Permittivity of free space or vacuum (F/m)

K_B = Boltzmann's constant (J/K)

T = Temperature (K)

q = charge of particle (C)

The size of Debye shield that is the plasma criterion is much smaller than Plasma size system.

The number of particles (Ion, Electron) in a Debye shield sphere (N_D) must be much greater than 1. The density of particles in Debye sphere can be defined by

$$N_D = \frac{4}{3} n_i \pi \lambda_D^3 \left(\frac{q^2}{m \epsilon_0} \right)^{1/2} \quad (2.2)$$

For N_D = Density of particles in Debye sphere (m^{-3})

n_i = Ion density (m^{-3})

λ_D = Debye Shield radius (m)

The particles in plasma respond electric field by adjusting their positions. The effect of this movement is to set up locale electric field within plasma that counteracts to apply. The frequency in which these oscillations occur is plasma frequency (ω_p). It is defined by

$$\omega_p = \left(\frac{n_i q^2}{m \epsilon_0} \right)^{1/2} \quad (2.3)$$

For ω_p = Plasma frequency (rad/s)

ϵ_0 = Permittivity of free space or vacuum (F/m)

n_i = Ion density (m^{-3})

q = charge of particle (C)

Plasma frequency (ω_p) that is the last plasma criterion is greater than $1/\tau$ when τ is the mean time between collision with neutral atom.

B. Equations of plasma

Particle Model Plasma can be completely described by five equations: four Maxwell's Equation and once the Lorentz Force. The first Maxwell's Equation is Poisson's Law describes the electric field produces by distribution of the electric charge. The Poisson's equation is

$$\nabla \vec{E} = \frac{q(n_i - n_e)}{\epsilon_0} \quad (2.4)$$

For \mathbf{E} = Electric field (V/m)

q = charge of particle (C)

n_i = Ion density (m^{-3})

n_e = Electron density (m^{-3})

ϵ_0 = Permittivity of free space or vacuum (F/m)

$$\vec{E} = -\nabla \phi \quad (2.5)$$

$$\nabla^2 \phi = -\frac{q(n_i - n_e)}{\epsilon_0} \quad (2.6)$$

C. Electron Density

Before proceeding further, it is well to review and extend our physical notions of "temperature." A gas in thermal equilibrium has particles of all velocities, and the most probable distribution. For simplicity, consider a gas in which the particles can move only in one dimension. (This is not entirely frivolous; a strong magnetic field, for instance, can constrain electrons to move only along the field lines.) The one-dimensional Maxwellian distribution is given by

$$f(u) = A \exp(-\frac{1}{2}mu^2 / K_B T_e) \quad (2.7)$$

Where $f(u)$ is the number of particles per cubic meter with velocity between u and $u + du$, $\frac{1}{2}mu^2$ is the kinetic energy, and K_B is Boltzmann's constant,

$$K_B = 1.38 \times 10^{-23} \text{ J}/\text{K} \quad (2.8)$$

The density n_e , or number of particles per cubic meter is given by

$$\int_{-\infty}^{\infty} f(u) du = n_e \quad (2.9)$$

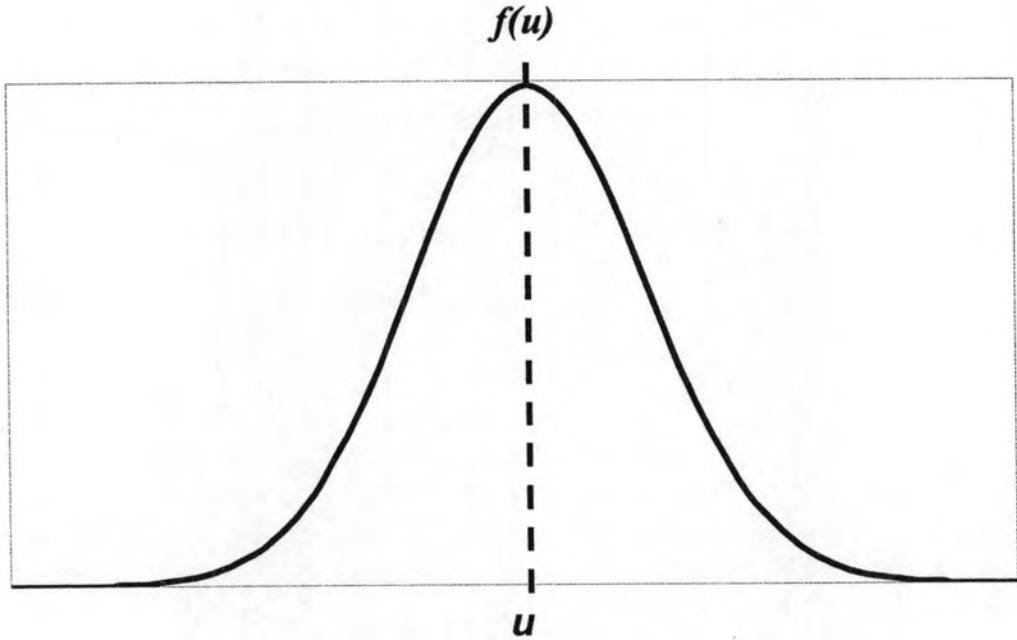


Fig. 2.5 A Maxwellian velocity distribution

The constant A is related to the density n_e by

$$A = n_e \left(\frac{m}{2\pi K T_e} \right)^{\frac{1}{2}} \quad (2.10)$$

In the presence of a potential energy (PE) that $PE = q\phi$, the electron distribution function is

$$f(u) = A \exp\left(-\frac{1}{2}mu^2 + q\phi\right) / K_B T_e \quad (2.11)$$

It would not be worthwhile to prove this here. What this equation says is intuitively obvious: There are fewer particles at places where the potential energy is large, since not all particles have enough energy to get there. Integrating $f(u)$ over u ,

$$\int_{-\infty}^{\infty} f(u) du = A \int_{-\infty}^{\infty} \exp\left(-\frac{1}{2}mu^2 + q\phi\right) / K_B T_e du \quad (2.12)$$

$$\int_{-\infty}^{\infty} f(u)du = 2A\sqrt{\pi} \left[\frac{2K_B T_e}{m} \right]^{\frac{1}{2}} \exp\left(-\frac{q\phi}{KT_e}\right) \quad (2.13)$$

$$\int_{-\infty}^{\infty} f(u)du = n_e \quad (2.14)$$

And

$$A = n_e \left(\frac{m}{2\pi K_B T_e} \right)^{\frac{1}{2}} \quad (2.15)$$

if ϕ is zero, n_e is plasma density (n_i).

$$n_e = n_i \exp\left(-\frac{q\phi}{K_B T_e}\right) \quad (2.16)$$

The second law Maxwell's Equation is the Faraday's Law of induction, which states the relationship between the magnetic field and electric field induces. The Faraday's Law of induction is

$$\nabla \times \vec{E} = -\frac{\partial \vec{B}}{\partial t} \quad (2.17)$$

For \vec{E} = Electric field (V/m)

\vec{B} = Magnetic induction or Magnetic flux density (Wb/m²)

t = Time(s)

The third Maxwell's Equation is Ampere's Law describes the magnetic field induced by current density and electric displacement. The Ampere's equation is

$$\nabla \times \vec{B} = \mu_0 \left(\vec{J} + \epsilon_0 \frac{\partial \vec{E}}{\partial t} \right) \quad (2.18)$$

For \vec{E} = Electric field (V/m)

\vec{J} = Current density (A/m²)

t = Time(s)

μ_0 = Permeability of free space (H/m)

ϵ_0 = Permittivity of free space or vacuum (F/m)

The last law Maxwell's Equation has no name which describes all magnetic field lines must be close. The last fourth Maxwell's Equation is

$$\nabla \vec{B} = 0 \quad (2.19)$$

For B = Magnetic induction or Magnetic flux density (Wb/m²)

The Lorentz Force equation explains the total force on particle due to its interaction with electric and magnetic field.

$$\vec{F} = q(\vec{E} + \vec{v} \times \vec{B}) \quad (2.20)$$

For \vec{F} = Force (N)

\vec{E} = Electric field (V/m)

q = charge of particle (C)

\vec{v} = Velocity (m/s)

\vec{B} = Magnetic induction or Magnetic flux density (Wb/m²)

A number of research activities in plasma source ion implantation are given below as the examples.

C. Liu, et al. [5] studied ion dynamics of pulsed plasma source ion implantation in the sheath of a hemispherical bowl-shaped target. This model is the temporal evolution of the pulsed plasma sheath during plasma source ion implantation is crucial as it affects the resultant surface properties and structures. In this paper two-dimensional fluid model is applied to the problem of computing ion dynamics in the sheath of a hemispherical bowl-shaped container. The potential in the sheath, the ion flux, dose distributions on the target surfaces are calculated by solving Poisson's equation and the equations of ion motion and continuity using finite difference methods. It is found that the differences in ion flux and dose along the inner, outer surfaces and the brim surface of the bowl exist.

X. B. Tian, et al. [6] studied in two-dimensional numerical simulation of non-uniform plasma immersion ion implantation. This model is the effectiveness of this approach depends on the uniformity of the incident ion dose. However, it is known that the lateral dose variation (non-uniformity) is less than optimal in some applications. Ion dose non-uniformity may lead to large variations in the biocompatibility for biomaterial

implants. Therefore, ion dose uniformity is an issue frequently investigated since the inception of PIII. Unfortunately, perfect dose uniformity is usually difficult to achieve when treating samples with a complex shape. The problem arises from the non-uniformity of the plasma density and self-consistent expansion of the plasma sheath. Concave surfaces frequently receive a smaller ion dose compared to convex surfaces since ions in a limited volume are competing for more surfaces and are depleted more readily. An effective solution is to produce non-uniform plasmas. For example, at the concave site, a higher plasma density may be helpful to weaken the ion competition and delay the depletion time. Consequently, the ion dose uniformity can be improved. In the work described here, we conduct two-dimensional numerical simulation of PIII into a trench target with the novel notion of non-uniform plasma.

B. Rauschenbach, et al. [7] studied about Plasma-sheath expansion around trenches in plasma immersion ion implantation. Plasma immersion ion implantation (PIII) has been developed as a fast and efficient surface modification technique of complex shaped three-dimensional objects. The temporal evolution of the potential surrounding the two-dimensional trenches during the PIII process is studied by a particle-in-cell simulation. The numerical procedure is based on the solution of the Poisson equation on a triangular grid and the determination of the movement of ions through the grid. A multi-level grid method is used for the solution of partial differential equation. The sheath evolution can be roughly divided into an ion-matrix phase (ions which are initially inside the trench are implanted) and a quasi-static expansion phase (ions enter the trench from the surrounding plasma starting at the receding sheath edge). The temporal potential evolution and the ion trajectories around trenches during the voltage pulse are demonstrated. This procedure leads to laterally resolved concentration distributions and implantation profiles, showing good agreement with experimental results.

B. Briehl, et al. [8] studied about Simulation of sheath and presheath dynamics in PIII. This Model studied the response of the sheath and presheath on the sudden negative charging of a planar electrode. In contrast to previous investigations, we started from an equilibrium sheath structure, rather than from homogeneous plasma. We obtained an improved description of the ion current density on the wall, the matrix sheath expansion and its dynamics.

S. Mandl, et al.^[9] studied about measured and calculated dose distribution for 2D plasma immersion ion implantation. Nitrogen was implanted into four cylinders (height 37 mm and diameter 4, 6, 8, and 12 mm) covered with aluminum foil using plasma immersion ion implantation at 30 kV. The homogeneity of the implantation, i.e. the spatial variation of the implanted dose, was determined for selected points on the top and the side walls of the cylinders with sputter depth profiling using Auger electron spectroscopy. Calculations approximating the dynamic sheath evolution with discrete sheath positions were performed to obtain the variation of the implanted dose and angle of incidence. Good agreement is found between the calculations and the experimental data. The ion dose exhibits a maximum on the top and decreases on the side walls. A second maximum is formed on the wall of the cylinder. The total dose variation is of the order of 50%.

K. C. Walter^[10] studied about Advances in PSII techniques for surface modification .Recent activities in plasma source ion implantation (PSII) technology include scale-up demonstrations for industry and development of variations on the original PSII concept for surface modification. This paper presents an overview of the continued growth of PSII research facilities world-wide and the industrial demonstrations within the USA. In order to expand the applicability of PSII, Los Alamos is actively researching a PSII-related technique called plasma immersion ion processing (PIIP). In one case, a pulsed-biased target can be combined with cathodic arc sources to perform ion implantation and coating deposition with metal plasmas. Erbium plasmas have been combined with oxygen to deposit erbia coatings that are useful for containment of molten metals. In a second case, hydrocarbon, inorganic and organometallic gases are utilized to create a graded interface between the substrate and the coating that is subsequently deposited by using pulsed-bias techniques. PIIP represents a significant advance since it allows coating deposition with all the strengths of the original PSII approach. Diamond-like carbon (DLC) and boron carbide are two such coatings that will be highlighted here for tribological applications.

Moreover, Plasma Source Ion Implantation: A New Approach to Ion Beam Modification of Materials was also studied by J. R. CONRAD^[4]. From such research, he found that Plasma source ion implantation (PSII) is a non-line-of-sight technique for

surface modification of materials which is optimized for ion implantation of non-planar targets in non-semiconductor no applications. In PSII, targets to be implanted are placed directly in a plasma source chamber and then pulse biased to high negative voltage (10-100 kV in our experiments). A thick ion matrix sheath forms around the target, and ions accelerate through the sheath drop and bombard the target from all sides simultaneously without necessity of target manipulation. Compared with conventional ion implantation, PSII minimizes the problems of shadowing and excessive sputtering of the target material, which can severely limit the retained dose of the implanted ion species. PSII has demonstrated (1) efficient implantation of ions to the concentrations and depths required for surface modification, (2) dramatic improvement in the life of manufacturing tools in actual industrial applications; (3) acceptable dose uniformity on non-planar targets without target manipulation and (4) that such uniformity can be achieved in a batch-processing mode. An examination of the comparative economics of surface modification by PSH relative to conventional ion implantation indicates substantial reductions in operating costs, by virtue of the greater throughput possible with PSII.

2.3. Ion Implantation and Ion Coating^[3]

When an ion penetrates through the medium, it loses some energy in many steps. The distance, in which the ion is able to move within the medium before it is totally stopped, is known as the ion range. This is an important parameter to be measured in many fields of nuclear physics such as the radiation detection and measurement, nuclear material, radiation damage, solid-state physics, semiconductor fabrication, the irradiation of the dosimetry, and many other nuclear applications. Traditionally, two methods are used to calculate the ion range. One is the Monte-Carlo method based on the concept of the stopping power. On the other hand, another method is to directly calculate the trajectory of the ion in the medium based on the model of its interaction with the medium.

The Monte Carlo method mainly concerns the macro-scale system. According to this method, the penetration range of an ion in a matter is represented by the averaged value from a numerous samplings. Without considering the effect of the lattices, the

needed time for the calculation is drastically reduced. A number of reports suggested that the method could be successfully applied for many problems. For example, H. Erramli, et al.^[11] were able to predict the ion range in an amorphous silicon material with a Monte Carlo computer code based on the stopping power concept. They found that the ions range evaluated for the energy of 10 keV to 10 MeV could be estimated with the standard TRIM/SRIM code. The TRIM/SRIM was originally designed by J. P. Biersack, et al.^[12]. It is often used for calculation of the physical quantities which related to the interaction between ion-beam and the materials, such as range and stopping power^[3, 4]. In this fashion, Monte Carlo method is, there for, commonly used for the studying regarding the ion transport in the matter. In general, based on the quantum mechanical treatment, the screened Coulomb collision interactions for the ion–atom collision together with the statistical algorithm one can be employed to calculate the stopping power. For this method, the entire medium is considered being absolutely amorphous, even when it is the lattice one. Since the model considers the medium being amorphous, it can not identity the effect of the lattice type. Beside, it also has its limit as it tends to predict the low implanting energy since it does not take the multiple interaction in to account.

With the molecular dynamic concept in stead of the Monte-Carlo concept, on the other hand, the lattice system receives more consideration. Still this method can only be calculated for the micro-scale system due to the time required for the calculation. The distribution of boron and hydrogen in HCP silicon was successfully simulated for the boron cluster implantation for shallow junction formation in the integrated circuits fabrication.

In this report, the ion range in the lattice medium was evaluated with the molecular dynamic concept and compared with the result obtained from the standard TRIM/SRIM model belonging to J. F. Ziegler^[13].

2.4 Ion Coating

The coating is a covering of the coating material on an object (substrate) to protect substrate or change its appearance. There are several types of coating methods for example the thermal process, the chemical process, the painting and the dipping process, the plating, the sputtering, the chemical vapor deposition (CVD), the physical vapor deposition (PVD), the plasma coating and the ion coating. In the case of the ion coating, the ions are accelerated by the sufficient energy to a target and they are buried into the surface basement material and then the coating layer grows from the inside of the substance until cover on the surface. In this research, the implantation model was modified to calculate the ion coating mechanisms. M. H. Shapiro, P. Lu^[14] employed the molecular dynamics (MD) techniques for the investigation of sputtering and other surface-modification processes. Moreover the experimental and molecular dynamics simulation comparisons of S. Zhang, et al.^[15] showed the friction behavior of hydrogenated carbon films. Their films were grown by reactive magnetron sputtering of graphite in argon hydrogen plasma. Beside, C. – J. Chu, T. – C. Chen.^[16] studied the film growing by the sputtering process with molecular dynamics (MD) simulation. The simulation of the film–substrate system at 500 K showed that thin films can also grow with two-dimensional layer-by-layer-like the way for larger size of substrate at room temperature. These simulated results are consistent with both earlier MD simulations and experimental observation.

2.5 Molecular Dynamic Calculation^[17]

The two atomistic simulation method are used most often are the molecular dynamics (MD) method and the Monte Carlo (MC) method. The molecular dynamic (MD) is emphasizes method because most of the atomistic simulations that are pertinent to forging have been molecular dynamics simulations. In either case, a computational cell of individual atoms is constructed and then operated on so as to simulate the properties and/or behavior of interest. The properties and behavior of crystal defects are the center

of interest. Although they used the same geometrical model of a solid, the computational operations involved in MD and MC simulation are qualitatively different. In the MD case, the computational operation consists of solving the atomic movement under the influence of the interatomic potential by Newtonian equations. In the MD case, the operational consists of exchanging the positions of two atoms at a time in accordance with Boltzmann statistics. Used in conjunction, the MD and MC methods provide a powerful means of analyzing phase transformations induced by stress and/or temperature manipulation, as in forging.

Computer simulation of material properties and behavior can be divided naturally into two classes: (1) continuum models and (2) atomistic models. In a continuum mode, the material concerned is regarded as a continuous medium. Most continuum simulations involve the solution of partial differential equations using either the finite-difference method or the finite-element method. In contrast, in an atomistic model simulation, the material concerned is regarded as an aggregate of individual atoms, and each atom is treated on an individual basis.

The Molecular Dynamic (MD) is a method for computational calculation in which the particles representing atoms, molecules, or ions are calculated for their movements under the influence governed by the law of physics. The result from MD simulation can describe and predict the consequence due to the atomic interactions, including their positions and velocities in the system at the microscopic level. MD calculation is based on Newton's second law for the calculation of the atom interactions. Therefore the important parameter which is required to calculate the atomic mechanisms is the atomic force. Even though there are a number of methods to determine the atomic force, one that is most commonly used is to specify the intermolecular potential then apply the Hamiltonian principle in order to determine the interacting force.

Neither an MD nor an MC simulation can be performed without the establishment of proper boundary conditions for the computational cell. There are four principal possibilities:

- a. Free-surface boundary
- b. Rigid boundary
- c. Flexible boundary

b. Periodic boundary

Normally, the computational cell contains 1000 to 20,000 atoms. As such it represents a very small speck of material, 600 atoms being a micro-femto-mole. The free-surface case pertains to a large, free molecule. Macroscopic crystals are simulated by using rigid, flexible, or periodic boundary conditions. In the rigid boundary case, a mantle of fixed-position atoms with the crystal structure of interest is placed around the computational cell. The thickness of the mantle is made larger than the range of the interaction between atoms. The mantle represents the part of the macroscopic crystal that can interact with atoms in the computational cell. The defect under study is contained in the computational cell.

The flexible boundary approach is more realistic than the rigid boundary approach in that the boundary region is capable of small atom displacements in response to forces exerted on it by atom at the perimeter of the computational cell. It has been shown that a rigid boundary can be used in studying point defects. However, certain types of simulations for extended defects require the use of flexible boundary conditions. Periodic boundary conditions are often used to simulate large systems. Roughly speaking, periodic boundary conditions simply mean that atoms at the extreme left of the cell. Similarly, atoms at the top of the cell interact with those at the bottom, and atoms at the front interact with those at the back. When periodic boundary conditions are used, the cell diameter must exceed twice the interaction range between two individual atoms.

In general, the capability of the periodic boundary condition approach has been vastly enlarged. As described above, the periodic boundary condition mode restricts the simulation to a computational cell with fixed volume and shape. As such, certain phase transformations can not be simulated. Recent developments allow changes in both the volume and the shape of the computational cell as the simulation proceeds when periodic boundary conditions are used.

For example, in a study of the ion implantation, the Molecular Dynamic calculation model can be used to model the interaction between the system constituents of the interaction (atoms and the implanting ions). The model assumes that the system constituents can be expressed in term of charge particles fixed charge points. Therefore, two types of particles are presented in the model. The first once is the implanting ion and

the second is atoms of the medium. It is assumed that both of particles interact due to the intermolecular interaction potential. Two kind of potential are to be employed. One is the long ranged electrostatic potential or coulombic potential. Another one is the short range called Lennard Jones Potential^[18, 19].

2.6 Interatomic Potential

2.6.1 Long Range Electrostatic (Coulombic) Potentials^[12, 13, 14, 20]

The principle of the interacting potential between an ion and the target atom is commonly described by the repulsive long ranged electrostatic (coulombic) potentials. This Coulombic potential must take the screening effect due to the surrounding electrons. The effect of the electrons can be simulated by adding a screening function controlled with dimensionless parameters to the coulombic potential. The screened potential functions called ZBL potential was proposed by Ziegler, Biersack and Littmark (J. F. Ziegler^[12, 13]) who used for this purpose.

Universal ZBL potential

The universal ZBL potential, one of the most commonly used screening potential functions in the ion implantation simulations, is related to the atomic masses Z_1 (ion) and Z_2 (target) by the expression

$$V_{ZBL} = \frac{1}{4\pi\epsilon_0} \left(\frac{Z_1 Z_2 q^2}{r} \right) \phi(r) \quad (2.20)$$

where q is electric charge, ϵ_0 is permittivity of the vacuum, and r is the interatomic distance between the ion and the atom. The universal screening function $\phi(r)$ is given by

$$\phi(r) = 0.1818e^{-3.2\frac{r}{a}} + 0.5099e^{-0.9423\frac{r}{a}} + 0.2802e^{-0.4029\frac{r}{a}} + 0.02817e^{-0.2016\frac{r}{a}} \quad (2.21)$$

where a_0 is Bohr's atomic radius and a is the modified Bohr's radius which is describe as

$$a = \frac{0.8854a_0}{Z_1^{0.23} + Z_2^{0.23}} \quad (2.22)$$

2.6.2 Short Range Potential [18, 19]

Lennard Jones Potential

As the ion and the atom come closer, the repulsive force known as Pauli repulsion, named for Pauli Exclusion Principle, becomes effective. To describe this force, a model called Lennard-Jones (LJ) potential was proposed in 1924. The model is a simple mathematical model representing the interaction between an atomic (ion) pair. Its functional form is described as

$$V_{LJ} = 4\epsilon \left[\left(\frac{\sigma}{r} \right)^{12} - \left(\frac{\sigma}{r} \right)^6 \right] \quad (2.23)$$

In this notation, ϵ is the depth of potential well and σ is the length parameter of the potential. It can be determined from the equilibrium positions of two atoms in lattice structure as.

$$\sigma = 2^{-1/6} R_{EQ} \quad (2.24)$$

R_{EQ} was lattice equilibrium position and ϵ or the cohesive energy can be determined by the method that show in following equation [21]:

$$\epsilon = \left| -\left(\frac{9e^2}{10} \right) \frac{1}{4\pi\epsilon_0 R_{EQ}} + \left[\frac{3}{10} \left(\frac{9\pi}{4} \right)^{\frac{3}{2}} \frac{\hbar^2}{m} \right] \frac{1}{R_{EQ}^2} \right| \quad (2.25)$$

Where

\hbar = Plank's constant

m = Atomic mass

These parameters can be described in this graph below.

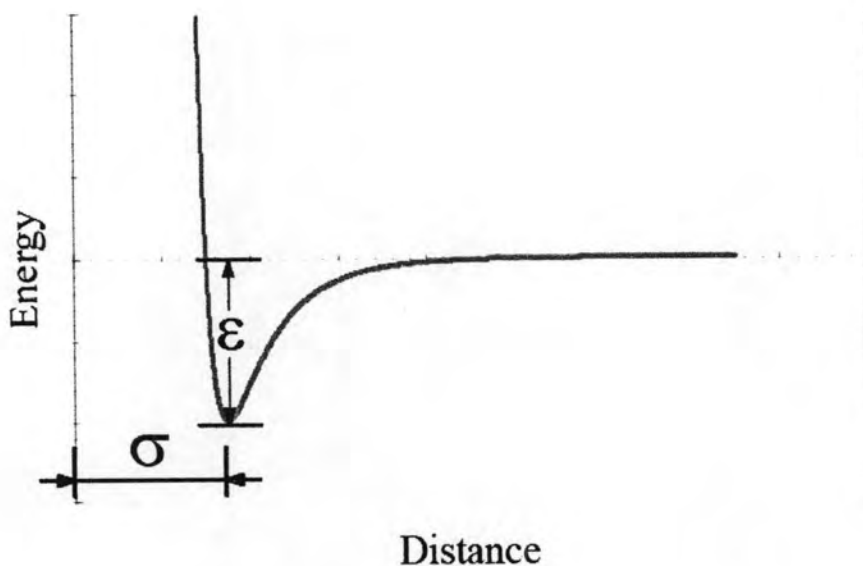


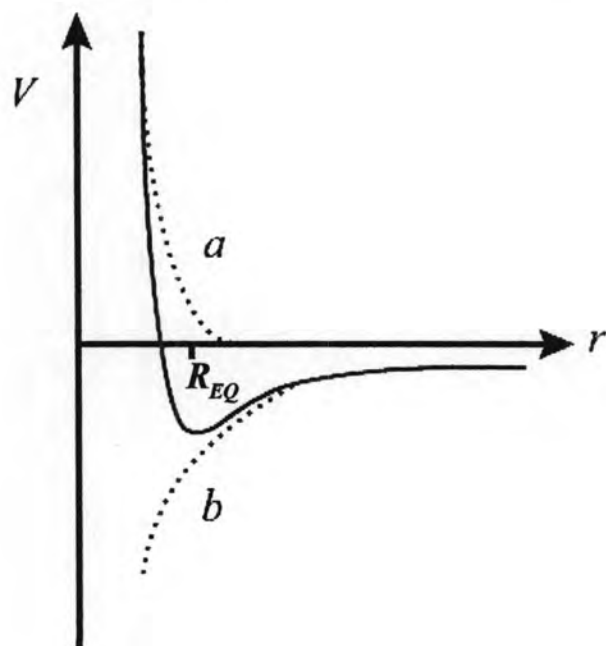
Fig. 2.6 The relationship between interatomic energy and distance in lattice system

For the $(1/r)^{12}$ term, this represents the Pauli principle. On the other hand, the $(1/r)^6$ term represents the effect at the longer range. In specific, this term represents the Van Der Waals dipole interaction.

However [22], there are several ideas about interatomic potential that show in table below. In the case of atoms, there is a charged nucleus surrounded by an electron cloud of opposite charge. It is evident that the potential function describing the interaction between atoms is far more complicated. Even in the simplest cases, $V(r)$ has never been determined exactly, but some simple considerations show that it must be dominated by two distinct contributions over the range of separation in which we are interested. Perhaps the simplest of all potential functions is the “hard-sphere” approximation. This potential is described as follows:

$$V(r) = \begin{cases} 0 & \text{for } r > r_0 \\ \infty & \text{for } r < r_0 \end{cases} \quad (2.26)$$

This potential function describes an interaction with an infinitely sharp cut-off at the atomic radius r_0 . At distances greater than this radius the interaction vanishes, while at distances less than r_0 the magnitude is infinity. This description is analogous to the behavior of billiard balls and hence, the atoms in this model are described as acting as such. Clearly this is not a very realistic description of atom–atom interaction since it was known that the electron shells can overlap.



Variation of interatomic potential with separation, r . Coulomb forces dominate at large separations (*b*) and the central repulsive force dominates at small separations (*a*), and at intermediate distances, there is a smooth transition between the two extremes with a minimum

Fig 2.7 corresponding to the equilibrium separation distance, R_{EQ} or D

Table 2.1 Interatomic potential

Potential	Equation for $V(r)$	Definitions
Hard-Sphere	$0 \quad ; r > r_0$ $\infty \quad ; r < r_0$	r_0 = Size of Atom
Born-Mayer	$Ae^{\left(\frac{r}{B}\right)}$	A, B determined from elastic moduli
Simple Coulomb	$\frac{Z_1 Z_2 q^2}{4\pi\epsilon_0 r}$	
Screened Coulomb	$\frac{Z_1 Z_2 q^2}{4\pi\epsilon_0 r} e^{\left(-\frac{r}{a}\right)}$	a Screening radius
Brinkman I	$\frac{Z^2 q^2}{4\pi\epsilon_0 r} e^{\left(-\frac{r}{a}\right)} \left(1 - \frac{r}{2a}\right)$	$a \cong \frac{a_0}{Z^{1/3}}$
Brinkman II	$\frac{AZ_1 Z_2 q^2}{4\pi\epsilon_0 \left(1 - e^{-Ar}\right)} e^{(-Br)}$	$A = \frac{0.95 \times 10^{-6}}{a_0} Z_{eff}^{1/6}$ $B = \frac{Z_{eff}^{1/3}}{Ca_0}$ $C \cong 1.5$
Firsov	$\frac{Z_1 Z_2 q^2}{4\pi\epsilon_0 r} \chi \left(\left[Z_1^{1/2} + Z_2^{1/2} \right]^{2/3} \frac{r}{a} \right)$	χ is screen function
TFD two-center	$\frac{Z^2 q^2}{4\pi\epsilon_0 r} \chi \left(Z^{1/3} \frac{r}{a} \right) - \alpha Z + \bar{\Lambda}$	
Inverse Square	$\frac{2E_R}{e} (Z_1 Z_2)^{5/6} \left(\frac{a_0}{r} \right)^2$	E_R = Rydberg Energy = 13.6 eV

At large separation, the principal interaction is supplied by the Coulomb forces while for smaller separations, the central field repulsive force is dominant. A similar

relationship applies to all crystals regardless of the nature of binding. In all cases there is a smooth curve with a minimum at the separation distance corresponding to the nearest neighbor distance in the lattice, R_{EQ} (also referred to as D). In describing the interaction between atoms, two yardsticks for points of reference was employed.

One is the Bohr radius of the hydrogen atom, $a_0 = 0.053\text{nm}$, which provides a measure of the position of the atomic shells. The other is R_{EQ} , the spacing between nearest neighbors in the crystal (typically $\sim 0.25\text{nm}$). When $r \ll R_{EQ}$, electrons populate the lowest energy levels (closed shells) of the individual atoms and only the outer valence shells will have empty levels. As two atoms are brought together, the valence shells begin to overlap and weak attractive forces such as van de Waals forces may develop. When $a_0 < r \leq R_{EQ}$ the closed inner shells begin to overlap. Since the Pauli Exclusion Principle demands that some electrons change their levels, and hence move to higher energy levels, the extra energy supplied in forcing the atoms together constitutes a positive potential energy of interaction. This is known as closed shell repulsion and the potential that most accurately describes this region is the Born–Mayer potential:

$$V(r) = Ae^{\left(\frac{r}{B}\right)} \quad (2.27)$$

Where A and B are constants determined from the elastic moduli. Although this function was first used by Born and Mayer to represent core ion repulsion in their theory of ionic crystals, it is perfectly valid for separations on the order of the equilibrium separation, R_{EQ} , and is useful in treatments of threshold or near-threshold collisions where the impact parameter is of the order R_{EQ} . When $r \ll a_0$, Coulomb interaction between the nuclei dominates all other terms in $V(r)$:

$$V(r) = \frac{Z_1 Z_2 q^2}{4\pi\epsilon_0 r} \quad (2.28)$$

At slightly larger distances, the nuclear charges are electro-statically “screened” by the space charge of the innermost electron shells that have entered the inter-nuclear space. The potential describing this behavior is known as the screened Coulomb potential:

$$V(r) = \frac{Z_1 Z_2 q^2}{4\pi\epsilon_0 r} e^{\left(\frac{r}{a}\right)} \quad (2.29)$$

Where $a = \frac{Ca_0}{(Z_1^{2/3} + Z_2^{2/3})^{1/2}}$ or

$$a = \frac{Ca_0}{(Z_1 Z_2)^{1/6}}$$

$$, C = 0.8853$$

and a_0 is the Bohr radius of the hydrogen atom. More generally, screening by the electron cloud is described by a screening function, $\chi(r)$ that is defined as the ratio of the actual atomic potential at a radius (r) to the Coulomb potential. The function of $\chi(r)$ is to moderate the Coulomb potential to describe the interaction between atoms at all separation distances. For large distances, $\chi(r)$ will tend toward zero, and at very small distances, $\chi(r)$ will tend toward unity. This is one way in which a single interatomic potential function can be used to describe all collisions. There are two description methods of regimes of interaction. At small separations ($r \ll a_0$) the screened Coulomb term dominates all others, with the screening effect decaying exponentially with the separation distance. In the region $a_0 < r \leq R_{EQ}$ electronic interaction dominates and is best described by the Born–Mayer potential. At intermediate separations there is no satisfactory description of the nature of atomic interaction. Unfortunately, it is exactly in this region where information is needed to provide a proper analytical description of radiation damage. Nevertheless, this idea may make a first approximation to the total potential by summing the controlling potentials at large and small separations:

$$V(r) = \frac{Z_1 Z_2 q^2}{4\pi\epsilon_0 r} e^{\left(\frac{r}{a}\right)} + A e^{\left(\frac{r}{B}\right)} \quad (2.30)$$

Where $A = 2.58 \times 10^{-5} (Z_1 Z_2)^{1/4}$ eV and $B = \frac{1.5a_0}{(Z_1 Z_2)^{1/6}}$ are empirical

formulae suggested by Brinkman, consistent with observed compressibility and elastic moduli in the noble metals Cu, Ag and Au. Unfortunately, there is a little experimental information about the forces between metal atoms, which is our primary interest. Figure 2.8 shows that the first term dominates for small separation and the second for large.

Brinkman suggested a model for the interaction between two identical atoms in which the nucleus is surrounded by a rigid charge distribution ρ_ϵ and it is assumed that both atoms supply a screened Coulomb field of the same type:

$$V(r) = \frac{Z^2 q^2}{4\pi\epsilon_0 r} e^{\left(\frac{-r}{a}\right)} \left(1 - \frac{r}{2a}\right) \quad (2.31)$$

This relation approaches the Coulomb repulsion as r approaches zero and changes sign at $r = 2a$, becoming a weak attractive potential with a minimum at $r = a(1 + \sqrt{3})$. However, this potential predicts strong interaction energy at large distances and may not represent the true physical picture for metals. Brinkman formulated a new potential function:

$$V(r) = \frac{AZ_1 Z_2 q^2}{4\pi\epsilon_0} \frac{e^{(-Br)}}{\left(1 - e^{(-Ar)}\right)} \quad (2.32)$$

Note that for small values of r the potential closely approximates the Coulomb repulsive interaction, i.e.,

$$\lim_{r \rightarrow \infty} V(r) \rightarrow \frac{Z_1 Z_2 q^2}{4\pi\epsilon_0} \quad (2.33)$$

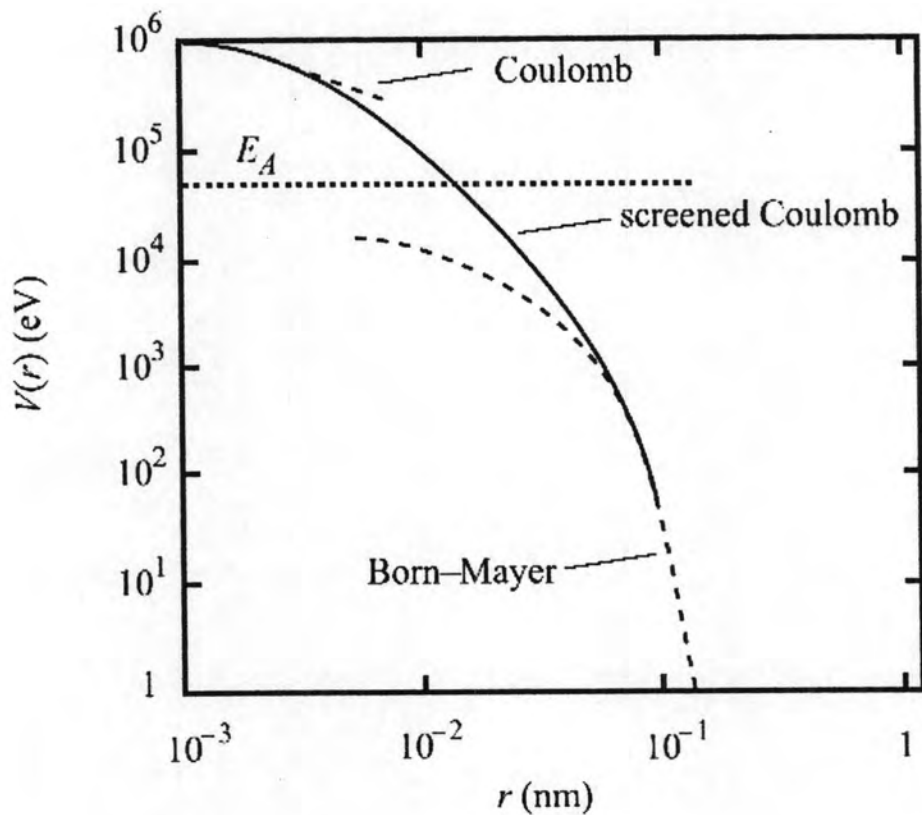


Fig. 2.8 Behavior of various potential functions over a range of separation distances between copper atoms

and at large separation, the potential equation approximates the exponential repulsion of the Born–Mayer type:

$$\lim_{r \rightarrow \infty} V(r) \rightarrow AZ_1Z_2e^{\left(-\frac{r}{B}\right)} \quad (2.34)$$

The constant B is defined as $B = \frac{Z_{eff}^{1/3}}{Ca_0}$, where $Z_{eff} = \sqrt{Z_1Z_2}$, and C is of the order 1.0 or 1.5. The constant A depends on the compressibility and bulk modulus, which depend on the overlap of closed electron shells. An empirical expression for A is

$$A = \frac{0.95 \times 10^{-6}}{a_0} Z_{eff}^{6/7} \quad \text{Substituting for } A, B \text{ and } C (= 1.5) \text{ into equation 2.32 gives:}$$

$$V(r) = 1.9 \times 10^{-6} Z_{\text{eff}}^{1/2} E_R \frac{e^{\left(\frac{Z_{\text{eff}}^{1/3} r}{1.5 a_0}\right)}}{1 - e^{\left(\frac{-0.95 \times 10^{-6} Z_{\text{eff}}^{1/7} r}{a_0}\right)}} \quad (2.35)$$

where $E_R = \frac{q^2}{4\pi\epsilon_0}$ is the Rydberg energy (13.6eV).

It should be noted that although the potential is a reasonably reliable function for all metals whose atomic number exceeds 25 over the range $r < 0.7 R_{EQ}$, it should not be used near $r = R_{EQ}$ since in the derivation it has been implicitly assumed that all interatomic distances are close to those of Cu, Ag and Au. It is therefore not a valid potential to use in calculating formation and migration energies of point defects.

Two other potentials should be discussed. The first is the Firsov or Thomas-Fermi two-center potential. This potential function is an improvement over the screened Coulomb potential by virtue of the fact it takes into account the change in electron energy connected with the mutual approach of the nuclei. The potential can be written as:

$$V(r) = \frac{\chi(r)}{r} \quad (2.36)$$

Where $\chi(r)$ is the screening function. In the case of the screened Coulomb potential:

$$\chi(r) = \chi_B(r) \text{ and}$$

$$\chi_B(r) = Z_1 Z_2 \frac{q^2}{4\pi\epsilon_0} e^{-\left(\frac{r}{a}\right)}$$

While in the Firsov potential:

$$\chi(r) = \chi_{TF} \left(\frac{r}{a} \right) = \chi \left(\left[Z_1^{1/2} + Z_2^{1/2} \right]^{2/3} \frac{r}{a} \right) \quad (2.37)$$

so that we have:

$$V(r) = \frac{Z_1 Z_2 q^2}{4\pi\epsilon_0 r} \chi \left(\left[Z_1^{1/2} + Z_2^{1/2} \right]^{2/3} \frac{r}{a} \right)$$

Where

$$\chi \left(\left[Z_1^{1/2} + Z_2^{1/2} \right]^{2/3} \frac{r}{a} \right) \text{ is a screening function.}$$

The second potential of interest is the Thomas–Fermi–Dirac two-center potential (TFD). The Thomas–Fermi–Dirac statistical model of the atom was employed to calculate a potential from first principles. As a consequence, this potential takes into account exchange effects and places a finite boundary, defined by r_b , on the spatial distribution of the electron cloud density ρ_e . The potential obtained for like atoms is:

$$V(r) = \frac{Z^2 q^2}{4\pi\epsilon_0 r} \chi \left(Z^{1/3} \frac{r}{a} \right) - \alpha Z + \bar{\Lambda} \quad (2.38)$$

where $\alpha = 3.16 \times 10^{-3} \frac{q^2}{4\pi\epsilon_0 a_0}$ and $\bar{\Lambda}$ is a set of integrals over exact single-center electron densities. Calculations using this potential have shown that for very small separations of less than $\sim 0.3a_0$, $V(r)$ agrees well with other theoretical curves and with experiment, while in the range $\sim 0.3a_0$ to $\sim 3.00a_0$, $V(r)$ agrees with other theoretical and experiment results better than the screened Coulomb potential or the Firsov potential.

In selecting the appropriate potential for a specific collision problem, the range of separation can be determined by equating the available kinetic energy to the potential and hence obtaining the smallest separation. The important interaction terms for the calculated separation can then be determined. For interactions between metal atoms at low kinetic energies, 10^{-1} to 10^3 eV, the Born–Mayer term alone is sufficient with constants given in equation 2.30. In cases of atom–atom collisions in the collision cascade, where energies from 10^3 to 10^5 eV are involved, an inverse power potential is extremely convenient. Such a potential can be formulated by fitting a function

$\frac{C}{r^s}$ (constant C) to one of the above potential functions over a limited range of r . For

example, one can fit an inverse square ($s = 2$) function to the screened Coulomb potential at $r = a$, obtaining the same slope, ordinate and curvature. This function is:

$$V(r) = \frac{Z_1 Z_2 q^2 a}{4\pi\epsilon_0 r^2} e^{-1} \quad (2.39)$$

when e is 1.66×10^{-19} .

For a limited range of r , this can be used as an approximate potential. Re-writing using the expression in equation 2.30 for a gives:

$$V(r) = \frac{2E_R}{e} (Z_1 Z_2)^{5/6} \left(\frac{a_0}{r} \right)^2 \quad (2.40)$$

A convenient alternative for numerical calculations uses the fact that $\frac{2E_R}{e} = 10eV$, hence:

$$V(r) = 10 (Z_1 Z_2)^{5/6} \left(\frac{a_0}{r} \right)^2 eV \quad (2.41)$$

This potential also applies to heavy ion bombardment in the energy range 10^3 to 10^5 eV. In the case of light ions at high energy, such as 5MeV protons, the simple Coulomb potential is adequate.

2.7 Two-body short-range interactions

When considering ionic materials, the Coulomb interaction is by far the dominant term and can represent, typically, up to 90% of the total energy. Despite having the simple form, just being given by Coulomb's law;

$$V(r)^{coulomb} = \frac{q_1 q_2}{4\pi\epsilon_0 r} \quad (2.42)$$

It is in fact the most complicated to evaluate for periodic systems (subsequently atomic units will be employed and the factor of $4\pi\epsilon_0$ will be omitted). This is because the Coulomb energy is given by a conditionally convergent series, i.e. the Coulomb energy is ill-defined for an infinite 3-D material unless certain additional conditions are specified. The reason for this can be readily understood - the interaction between ions decays as the inverse power of $4\pi\epsilon_0$, but the number of interacting ions increases with the surface area of a sphere, which is given by $4\pi\epsilon_0 r^2$.

After the Coulomb energy, the most energy contribution is usually the dispersion term. From the quantum theory we know that the form of the interaction is a series of terms in increasing inverse powers of the interatomic distance, where even powers are usually the most significant:

$$V(r)^{\text{dispersion}} = -\frac{C_6}{r^6} - \frac{C_8}{r^8} - \frac{C_{10}}{r^{10}} - \dots \quad (2.43)$$

The first term represents the instantaneous dipole - instantaneous dipole interaction energy, and the subsequent terms correspond to interactions between higher order fluctuating moments. Often in simulations only the first term, $\frac{C_6}{r_{ij}^6}$, is considered as the dominant contribution.

Again, the dispersion term can cause difficulties due to the slow convergence with respect to a radial cut-off. Although the series is absolutely convergent, unlike the Coulomb sum, the fact that all contributions are attractive implies that there is no cancellation between shells of atoms.

Contributions to the energy must be included with represent the interaction between atoms when they are bonded, or ions when they are in the immediate coordination shells. For the ionic case, a repulsive potential is usually adequate, with the most common choices being either a positive term which varies inversely with distance, or an exponential form. These lead to the Lennard-Jones and Buckingham potentials, respectively, when combined with the attractive C_0 term:

$$V(r)^{\text{Buckingham}} = Ae^{-\left(\frac{r}{\rho}\right)} - \frac{C_6}{r^6} \quad (2.44)$$

$$V(r)^{\text{Lennard-Jones}} = \frac{C_m}{r^m} - \frac{C_6}{r^6} \quad (2.45)$$

The Buckingham potential is easier to justify from a theoretical perspective since the repulsion between overlapping electron densities, due to the Pauli principle, which take an exponential form at reasonable distances. However, the Lennard-Jones potential, where the exponent is typically 9-12, is more robust since the repulsion increases faster with decreasing distance than the attractive dispersion term. For covalently bonded atoms, it is often preferable to Coulomb subtract the interaction and to describe it with either a harmonic or Morse potential. In doing so, the result is a potential where the parameters have physical significance. For instance, in the case of the Morse potential the parameters become the dissociation energy of the diatomic species, the equilibrium bond length and a third term, which coupled with the dissociation energy, is related to the vibrational frequency for the stretching mode. This does not represent an exhaustive list of the forms used to describe short range interactions, but most other forms are closely related to the above functional forms, which consists of tabulation of function values versus distance. A full list of the two-body potential functional forms presently available is given in Table 2.2.

Table 2.2 Functional forms for two-body interatomic potentials

Potential Name	Formula	Units of Input
Buckingham	$Ae^{(-r/\rho)} - C_r^{-6}$	A in eV, ρ in Å, C in eVÅ ⁶
Lennard-Jones [†]	$A_r^{-m} - B_r^{-n}$ or $\epsilon \left(c_1 \left(\frac{\sigma}{r} \right)^m - c_2 \left(\frac{\sigma}{r} \right)^n \right)$ $c_1 = \left(n/(m-n) \right) (m/n)^{(m/(m-n))}$ $c_2 = \left(m/(m-n) \right) (m/n)^{(n/(m-n))}$	A in eVÅ ^m , B in eVÅ ⁿ , ϵ in eVÅ ⁶ , σ in Å
Harmonic*	$\frac{1}{2}k_2(r - r_0)^2 + \frac{1}{6}k_3(r - r_0)^3 + \frac{1}{12}k_4(r - r_0)^4$	k_2 in eVÅ ⁻² , r_0 in Å, k_3 in eVÅ ⁻³ , k_4 in eVÅ ⁻⁴
Morse	$D \left\{ \left(e^{(-a(r-r_0))} \right)^2 - 1 \right\}$	D in eV, a in Å ⁻² , r_0 in Å
Spring (core-shell)	$\frac{1}{2}k_2r^2 + \frac{1}{24}k_4r^4$	k_2 in eVÅ ⁻² , k_4 in eVÅ ⁻⁴ ,
General	$Ae^{(-r/\rho)r^{-m}} - C_r^n$	A in eVÅ ^m , ρ in Å, C in eVÅ ⁿ
Stillinger-Weber(sw2)	$Ae^{(\rho/(r-r_{\max}))} (B_r^{-4} - 1)$	A in eV, ρ in Å, B in eVÅ ⁴

[†] combination rule promise

* k_3, k_4 are optional

2.8 Particle Damping and Static Equilibrium Atom Position Calculations^[17]

As each coating ion travels through the medium, it interacts with the nuclei in the medium and gradually loses its kinetic energy. Eventually the ion will slow down and is eventually trapped in the medium. To simulate this process, the Molecular Dynamic simulation is used to calculate the trajectory of an ion in the lattice medium.

In this study, the static equilibrium was calculated first and then set that point for the MD simulation to reduce the consumed simulation time. This point resembled with the real static equilibrium and gave the accuracy result because this study concerned mean value only.

In order to reduce the time and resources required for the simulation, it was necessary to stop the motion of an ion at the appropriate time. Two possible methods for the artificial damping on the motion of an ion could be used; one was the *quasidynamical method* and the other was *the localized damping* or the *microconvergence method*. For this study, the microconvergence method was implemented.

The simplified microconvergence method implemented for the calculation resulted in the damping force \vec{F}_D that was written as

$$\vec{F}_D = K\vec{v} \quad (2.46)$$

This above relation shows the proportional relationship between the damping force (\vec{F}_D) and the ion's velocity (\vec{v}) that corresponded to the ion's kinetic energy. With the damping force, it was now possible to force the particle to slow down and finally trapped in the medium under the given period for the calculation.

There are two types of atomic interaction potentials between the coating ion and lattice atoms were implemented. One was ZBL potential for the long range interaction and the other one was LJ potential for the short range. The interaction force between the ion and lattice atoms was determined by Hamiltonian function (H) where

$$H = \frac{1}{2m} P^2 + f_{IPE}(x, y, z) \quad (2.47)$$

The $f_{IPE}(x, y, z)$ is the interatomic force between the ion and lattice atoms. When the earlier ions batches are accelerated into the target material, the coating over the target did not immediately happen. The ions would travel through the target's network of lattices up to a specific depth and then was trapped. The following equation described the process,

$$\vec{F} = -\nabla H^{lattice} - \sum_{N=0}^n \nabla H_N^{implanted\ ion} + \vec{F}_D \quad (2.48)$$

For the above equation, \vec{F} was the interatomic force, $\nabla H^{lattice}$ was the interacting forces between the ion and lattice atoms, $\sum_{N=0}^n \nabla H_N^{implanted\ ion}$ is the summation of the interacting force between the ion and n is previously trapped ions.

For the latter ions batches, the more interaction force represented by the increasing of the $\sum_{N=0}^n \nabla H_N^{implanted\ ion}$ parameter would effect to the ions. The increasing of that parameter affected the reducing of the total interatomic force reasonable so that the ions could not travel to the lattice medium as deep as the previously one. With the certain interatomic force, the ions would not travel into the lattice medium that caused the covering at the surface named the coating process.

2.9 Trajectories Calculation and Analysis on Coating Process

Based on the concept of Hamiltonian system and the artificial damping, the force acting on the coating ion was described as

$$\vec{F} = -\nabla H + \vec{F}_D \quad (2.49)$$

With the microconvergence model, the above equation was written as

$$\vec{F} = -\nabla H + K\vec{v}(x, y, z) \quad (2.50)$$

In the Cartesian coordinate, the equation became

$$\vec{F} = - \left(\frac{\partial f_{IPE}(x, y, z)}{\partial x} \hat{i} + \frac{\partial f_{IPE}(x, y, z)}{\partial y} \hat{j} + \frac{\partial f_{IPE}(x, y, z)}{\partial z} \hat{k} \right) + K(v_x \hat{i} + v_y \hat{j} + v_z \hat{k}) \quad (2.51)$$

For the above relation, K was the coefficient that the suitable value for the calculation must be obtained. In general though, K has the negative value where magnitude depended much on the type and configuration of the target, the type of the ion and its energy level. For this study, K was obtained by simply matching the calculation of the penetration length with the result from the conventional code TRIM/SRIM.

For the calculation, the integration at each time steps was done with Runge-Kutta technique and the periodic boundary condition was assumed for the system.

To test the concept, the system of interest had the coating of the target whose the mass number was 56 and the atomic number was 26 by the ions whose the mass and the atomic number were 195 and 78. The crystalline structures of target were figured to either SC, BCC or FCC. Such configurations were chosen because of the large values of the mass and the atomic numbers. This allowed their effects on the potential field, which governed the interaction forces, to be clearly demonstrated. At the same time, such configurations were common enough that they could be examined and compared by TRIM/SRIM code. In addition, the heavy ion had high energy lost ratio due to the interaction with the matter but with the small angle of scattering. Such condition allowed the comparison between the obtain results from the simulation with that for TRIM/SRIM to be more possible. Each simulation was conducted for 3000 time steps, whose time step 10^{-17} - 10^{-15} s were implemented. The results obtained were then analyzed.

As mentioned before, there are 3 layers in the coating material. The study divided those layers by the concept of the ion range. The mixed layer started from the upper surface of the target material to the ion range within the material. Above that layer was the coating layer started from the upper surface outside of the target material in the opposite direction with the ion range. For the sustaining or the basement layer, the layer was inside the target material defined from the ion range to the lower surface of the material.

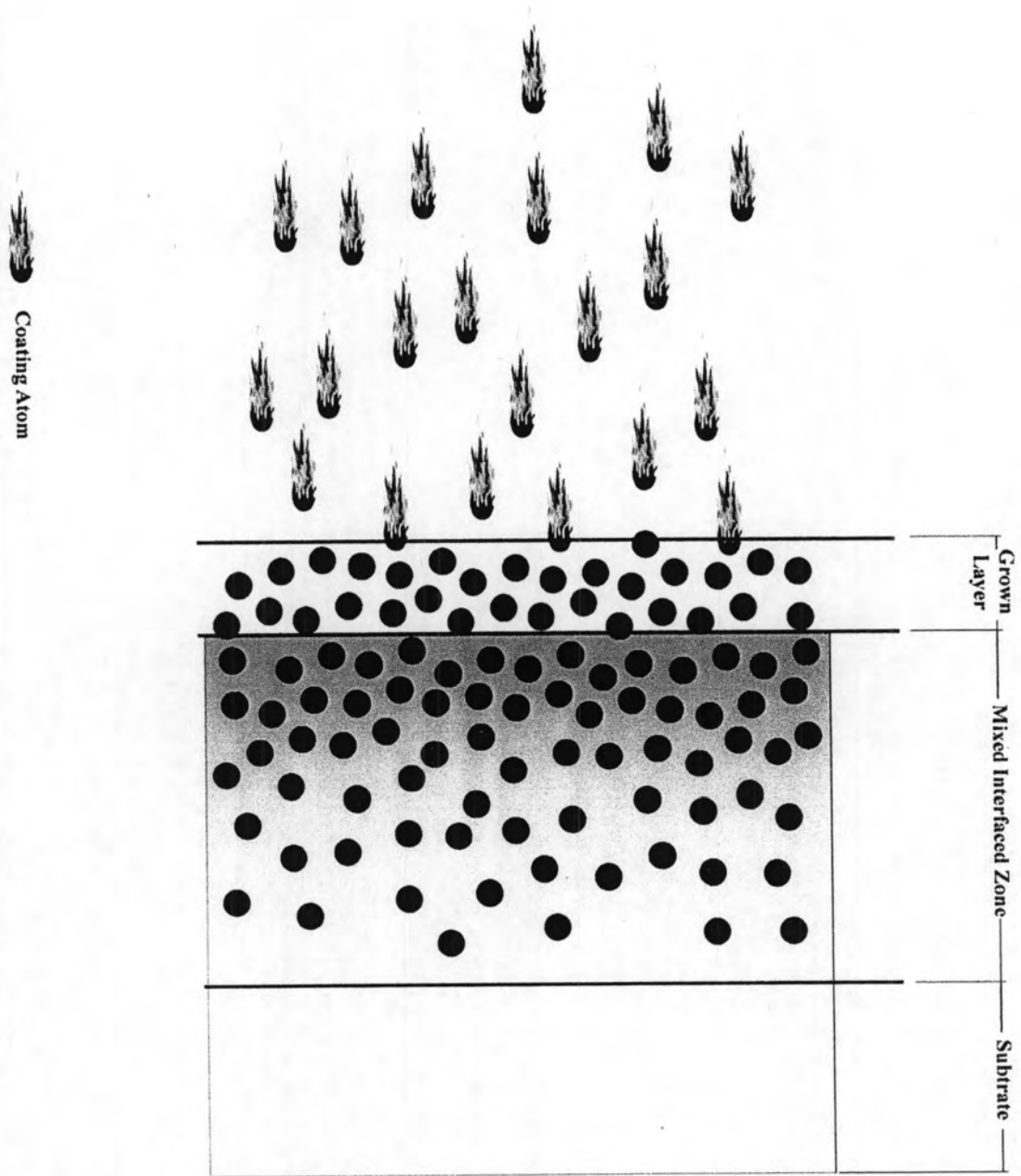


Fig. 2.9 characteristic of layer in coating model

2.10 SRIM/TRIM Model^[23]

SRIM (The Stopping and Range of Ions in Matter) is a set of programs used to calculate the stopping and range of ions into matter using a quantum mechanical treatment of ion-atom collisions. The calculation made by the use of statistical algorithms, allowing the ion to jump between calculated collisions, and then averaging the collision results over the intervening gap. So this calculation is very efficient. During the collisions, the ion and atom have a screened Coulomb collision, including exchange and correlation interactions between the overlapping electron shells. The ion has long range interactions creating electron excitations and plasmons within the target. These are described by including a description of the target's collective electronic structure and interatomic bond structure when the calculation is setup. The charge state of the ion within the target is described using the concept of effective charge, which includes a velocity dependent charge state and long range screening due to the collective electron sea of the target.

TRIM (the Transport of Ions in Matter) is the most comprehensive program included. TRIM will accept complex targets made of compound materials with up to eight layers, each of different materials. It will calculate both the final 3D distribution of the ions and also all kinetic phenomena associated with the ion's energy loss: target damage, sputtering, ionization, and phonon production.

This code is basically a calculation of Monte Carlo. One projectile at a time is incident on a solid surface. The projectile in solid medium interaction process is shown below

- Only two-body collisions are considered
- The computation treats a three dimensional array of atoms in the solid, but does not consider crystallography. That is, the solid is assumed amorphous.
- Specific crystallographic effects (focusing or channeling) are not treated.
- The accumulation of damage (cascade overlap) is not treated.
- The target may consist of multiple layers, each containing several different elements.

The SRIM program originated in 1983 as a DOS based program. For those used to TRIM (DOS), the SRIM package contains the last version of TRIM (1998). SRIM-2000 is the new version which requires a PC with any Windows operating system. Everyone can download from www.srim.org.

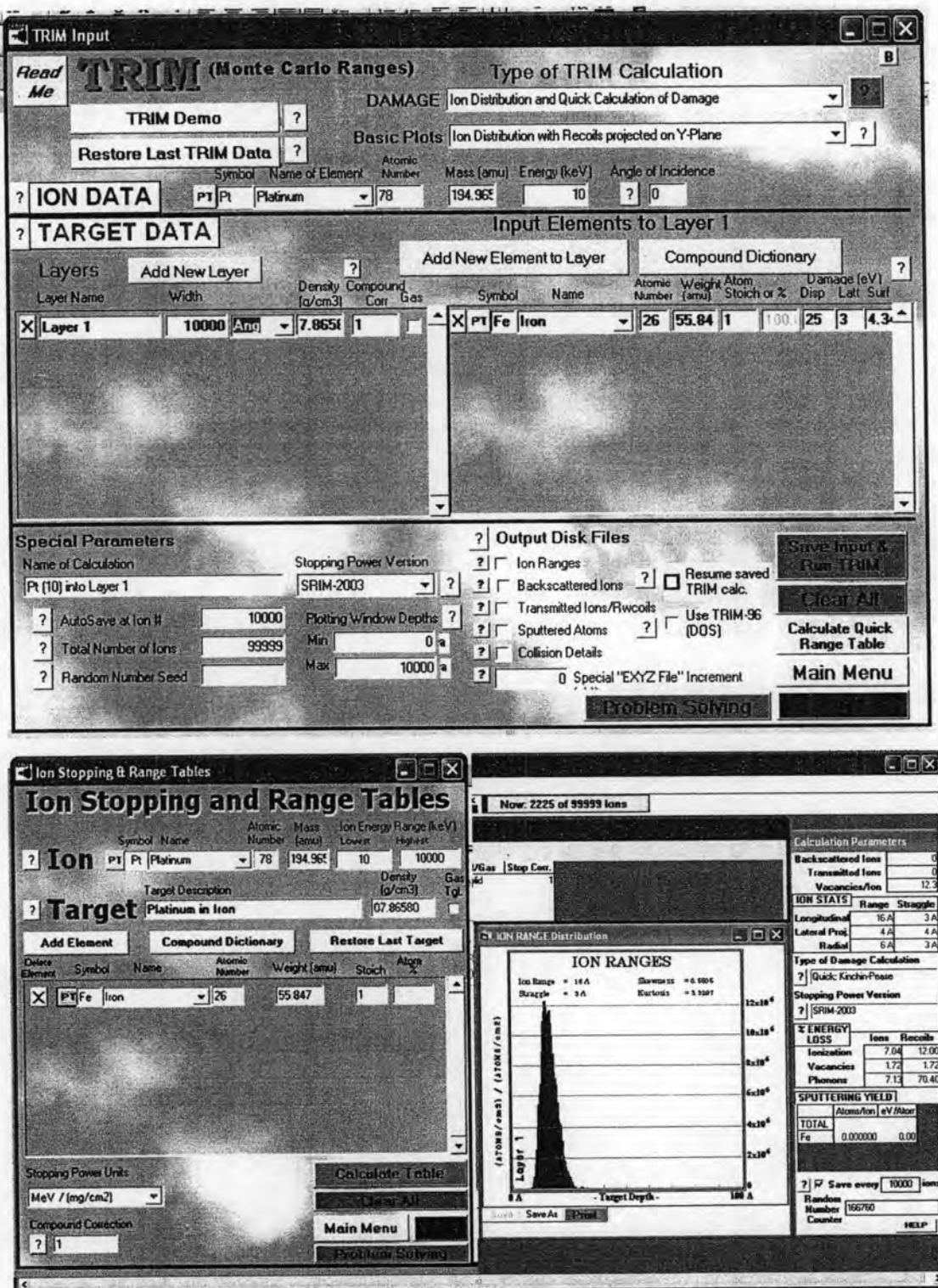


Fig. 2.10 SRIM/TRIM model Interface